A multiscale framework for the evaluation of thermal conductivity of sintered powder at the powder bed fusion with electron beam conditions

Progress in Additive Manufacturing
https://doi.org/10.1007/s40964-023-00558-w

FULL RESEARCH ARTICLE

A multiscale framework for the evaluation of thermal conductivity of sintered powder at the powder bed fusion with electron beam conditions

Giovanni Rizza[1] · **Manuela Galati**[1] · **Luca Iuliano**[1]

Received: 30 May 2023 / Accepted: 25 December 2023

Abstract
The thermal conductivity of the powder bed during the electron beam powder bed fusion (PBF-EB) process strongly influences the process conduction and the quality of the components produced. The evaluation of this property is challenging. The models currently available in the literature cannot provide values of the thermal conductivity that consider the temperature evolution typical of the preheating step. This work presents a novel computational framework to evaluate the thermal conductivity of a powder bed for the PBF-EB process. The framework combines the thermal conditions of the PBF-EB process with information on the geometrical features of the powder bed and an analytic method to calculate the thermal conductivity and its variation with temperature and time. The proposed numerical framework is applied to the body centred structure (BCC), a typical arrangement that can emulate the PBF-EB conditions. The numerical framework is multiscale by nature, providing information about the whole powder bed starting from geometrical information about the neck among the powder particles.

Keywords Thermal conductivity · Powder bed · Numerical modelling · Electron beam melting · Tortuosity · Neck

1 Introduction

The quality of parts produced using the powder bed fusion additive manufacturing process is strictly related to the powder bed characteristics [1]. Thermal characteristics of the powder bed, such as emissivity or thermal conductivity, need to be considered as a further process variable that increases the process complexity [2]. Thermal conductivity influences the interaction between the energy source and the powder [3], the heat transfer phenomena during the whole process [4] and the cooling rate with a direct influence on the component microstructure [5]. Moreover, the powder material's thermal conductivity influences the manufactured components' surface quality in the overhang and cellular structures [6]. In the case of the powder bed fusion with electron beam (PBF-EB), heat transfer occurs within partially sintered powder mainly because of thermal conductivity among the particles. Other heat transfer mechanisms are negligible because the process occurs under a vacuum (no convection [7]), and the contribution of radiation is an order of magnitude smaller than the conductive counterpart within solid material [8]. The powder particles' packing structure also influences thermal conductivity. In the PBF-EB process, the powder size distribution ranges between 45 and 105 µm. This powder size distribution generates a disordered packing structure. The temperature increases during the preheating and the high temperature during the whole process activates diffusion phenomena. These phenomena produce a bridge of material at the contact point between the powder particles, usually identified as the neck. Hence, if the temperature and the neck evolution are considered, evaluating the powder bed's thermal conductivity remains challenging. To reduce the complexity of the thermal conductivity evaluation, several works consider simplified packing structures for the powder bed, such as a body centred cubic (BCC) [7, 9].

The thermal conductivity of the powder material is mainly investigated by considering experimental or numerical approaches. An overview of the experimental approaches was proposed by Presley and Chreistensen [10]. Some of the experimental methods are dedicated to the PBF-EB process [11–14]. However, some proposed methodologies neglected

✉ Giovanni Rizza
giovanni.rizza@polito.it

[1] Department of Management and Production Engineering (DIGEP), Integrated Additive Manufacturing Center (IAM@PoliTo), Politecnico di Torino, Corso Duca degli Abruzzi 24, 10129 Turin, Italy

Published online: 08 February 2024

the vacuum environment that characterises the PBF-EB process [14]. Other works investigated the thermal conductivity at different temperatures but neglected the influence of the high temperature on the evolution in time of the neck that connects the powder particles [11, 12].

Among the different numerical models for thermal conductivity available in the literature, some are dedicated to additive manufacturing techniques [9, 15, 16]. Gusarov et al. [9] proposed a numerical model for the powder bed fusion with the laser beam process for polymers (PBF-LB/P). In this case, the thermal conductivity of bulk material was scaled according to the relative density of the powder bed, the coordination number, and the dimension of the neck between the powder particles. However, the geometrical information required to implement this model constrains the validity of this model to simplified structures of the powder bed, such as the simple cubic (SC), face centred cubic (FCC), or body centred cubic (BCC) structures, where these parameters are easy to measure. Chua et al. [15] implemented a finite element (FE) model consisting of a couple of powder particles in contact at a point to investigate the thermal conductivity as a function of the dimension of the bridge of material (neck) among the powder particles. The simulations were conducted considering processing conditions representative of the PBF-EB conditions: air at low pressure around the powder particles, powder particles with a diameter of 50 µm and a temperature that varied between 0.4 Tm and the solidus temperature of the material. The results obtained for a couple of powder particles were extended to a powder bed by linear interpolation but without considering the actual geometry of the powder bed. To overcome such approximation in the case of micro PBF-LB/P, Grose et al. [16] used a PF simulation to predict the neck evolution during the process, and a FE model to perform a steady state heat transfer simulation and evaluate thermal conductivity. This methodology is computationally expensive and required several adjustments to move from the sintering simulation to the thermal conductivity. Moreover, the connection of phase field simulation to the AM process remains unclear, as the material parameters and the temperature evolution to set up the PF simulation were not provided.

In the case of a powder bed, determining the thermal conductivity of the solid fraction requires knowledge of the heat transfer region. For partially sintered powder particles, this area must consider a net of connected particles. Therefore, it could be necessary to describe, in some way, the complexity of the path within the material. A similarity may be found in the concept of the tortuosity index. This index is usually used to describe the flow of a fluid through the void of a porous media. However, this index was only recently proposed as a methodology to investigate the thermal or electrical diffusion phenomena in a porous material. Ahmadi et al. [17] proposed an approach based on volume averaging to evaluate the tortuosity of mono sized arrays of spheres. In this case, tortuosity was evaluated as a flow within the material's pores. The methodology was adopted to evaluate the tortuosity of regular cubic and tetrahedral structures of spherical powder particles. The results were in good agreement with both theoretical and experimental literature data. Montes et al. [18] proposed the evaluation of thermal tortuosity as the ratio between the sample length in the heat flux direction and the length of the shortest path within the solid material that connects the extremes of the sample. However, in the case of a powder substrate with low density, the dimension of the solid connection between the powder particles was neglected [18]. Leung et al. [13] used an analysis of the tortuosity factor to evaluate the thermal conductivity. The value of the tortuosity factor was obtained using an open source application, TauFactor [19]. The software takes as inputs the cross-section images of the porous media that, in this case, were tomograms of the sintered powder bed. Then, the software applied a heat flux on a subvolume of the powder image, at the top of the picture, and the thermal flux was followed along the conductive phase. The results were strictly bonded to the image adopted for the evaluation, the dimension of the inlet area and the balance between the phases of the system. Moreover, the sintered test samples were not representative of the evolution of geometry during the sintering process of the PBF-EB process.

The current work proposes a novel methodology to evaluate the thermal conductivity of a powder bed at the PBF-EB conditions based on evaluating tortuosity within the solid material of a REV with a BCC packing structure. This methodology attempts to overcome the limitations of the current literature considering the vacuum, the temperature changes and the evolution of the neck among the powder particles during the PBF-EB process.

2 Methodology

The thermal conductivity of a powder bed can be evaluated as a function of the thermal diffusivity of the powder, as reported in Eq. (1) [12]

$$\lambda_{pow}=\alpha_{pow}\rho_{pow}c_p \tag{1}$$

where α_{pow} represents the thermal diffusivity of the powder material, ρ_{pow} represents the density of the powder bed, and c_p represents the specific heat capacity of the powder bed.

ρ_{pow} can be evaluated as $\rho_{pow}=\rho_0 n$, where ρ_0 is the theoretical density of the bulk material considered and n represents the volume fraction of the solid material within the considered domain.

α_{pow} can be expressed as reported in Eq. (2) [13]

$$\alpha_{pow}=\alpha_0\frac{n}{\tau} \tag{2}$$

in which α_0 represents the thermal diffusivity of the bulk material and τ represents the tortuosity of the system.

The tortuosity is an inherent feature of a porous material that, originally, was developed to describe the complexity of a flux path within the voids. The simplest way to measure the tortuosity is, therefore, the ratio between the length of the tortuous flow path within the pores of the material (L_r) and the shortest distance between the inlet and outlet section of the flux (L_d). The more L_r differs from L_d, the more the path to cover is complex.

In the case of a powder bed and the application of the tortuosity concept to a thermal problem, the scenario is different. The heat flows within the solid material of the net formed by sintered particles when referring to the heat transfer problem. As an example, Fig. 1 shows schematically the ideal concept of tortuosity applied to a 2D section of a powder bed composed of randomly distributed particles in which the neck between neighbouring particles is already formed. The red line in Fig. 1 highlights one of the possible paths for the heat flow throughout the particles connected by the neck. As can be observed, the length of the actual path within the solid material (L_r in Fig. 1) is longer than the thickness of the section (L_d in Fig. 1).

The measure of L_r is non-trivial because, in complex structures, multiple heat flow paths within the solid material may be created. To overcome this issue, Ahmadi et al. [17] proposed an innovative formulation for fluid flow within voids, in which the tortuosity is calculated as a macroscopic property of the material, considering only the geometrical characteristics of the structure. This formulation has been adapted in this work to provide a new formulation for the tortuosity valid for the heat path within a bulk material consisting of a net of sintered particles. Even if the nomenclature has been formally kept analogous to the one proposed by Ahmadi et al. [17], the hypothesis and the physical meaning of each term are valid only for determining the tortuosity of a net of particles. Equation 3 reports the calculation of τ under the following hypotheses:

- The porous material is made of two phases: a persistent solid phase and the void space between the solid particles.
- The solid phase is distributed heavenly over the domain.
- The phases where the flux occurs should be connected. This means that any two points inside the conducting phase should be linked by a curve that is entirely contained within the conducting phase.

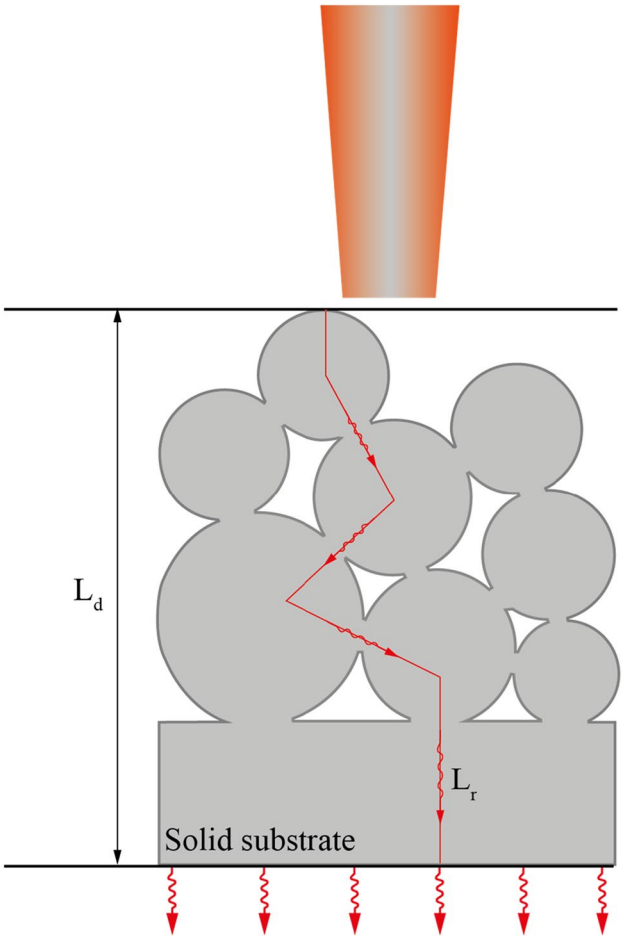

Fig. 1 Scheme of a partially sintered powder structure under the action of the electron beam. The red line within the powder particle represents one possible heat flow path from the inlet to the outlet section. L_r represents its length. L_d represents the straight distance between the inlet and the outlet

$$\tau=\sqrt{\frac{n^2d_p^2}{36(1-n^2)}\frac{(2+T_f^*)}{3\Delta_f^2T_f^*}} \tag{3}$$

For the definition of the quantities presented in Eq. (3), it is necessary to define a domain for the calculation called representative elementary volume (REV). The main characteristic of the REV is that the distribution of the solid material and the void is statistically representative of the powder bed.

Within the REV, n represents the volume fraction of the solid material with respect to the total volume (Eq. (4)); Δ_f represents the hydraulic radius defined as the ratio of the volume of the solid material and the void-solid interface area (Eq. (5)). T_f* represents the tortuosity tensor of the fraction of volume occupied by the solid material. For an isotropic medium, this can be written as in Eq. (6), where δ_{ij} is the Kronecker delta function and $\theta^S=S_{ss}/S_0$.

$$n = \frac{U_{0S}}{U_0} \tag{4}$$

$$\Delta_f = \frac{U_{0S}}{S_{fs}} \tag{5}$$

$$T_f^* = \frac{\theta^S}{n}\delta_{ij} = \frac{S_{SS}U_0}{S_0 U_{0S}}\delta_{ij} \tag{6}$$

U_{0S} represents the volume of the solid material within the REV and U_0 represents the total volume of the REV.

S_{fs} represents the interface area between the solid material and the vacuum inside the REV.

S_{SS} represents the area of the material that crosses the REV boundaries, while S_0 represents the total lateral surface of the REV.

U_0 and S_0 are evaluated as the volume and surface of the minimum convex polygon or convex hull [20] that contains all the centres of the powder particles and represents the REV.

Assuming a generic REV, the volume of the solid phase contained on the inside (U_{0s}) was evaluated as reported in Eq. (7)

$$U_{0S} = \iint_{D_{0S}} f(x,y)\, dD_{0S} \tag{7}$$

where x and y represent the coordinates of the plane that contains the generic function $f(x,y)$ that describes the boundaries of the solid material and the integration domain (D_{0S}). $f(x,y)$ can be determined assuming that the sintering structure is made of spherical powder particles connected by the neck that can be approximated by a one sheet hyperboloid. The interface area of solid material to the void, $S_{fS,}$ was evaluated as reported in Eq. (8), assuming that the geometry of the solid material is axisymmetric.

$$S_{fS} = \vartheta \int_a^b g(x)(1 + (g'(x)^2))dx \tag{8}$$

where ϑ is the rotation angle, a and b represent the extreme of integration and $g(x)$ represents the function that describes the profile of the solid material. This profile was considered as the sum of the segment of a circle representing the powder particle and a hyperboloid representing the neck. $g'(x)$ represents the first order derivative of $g(x)$.

Finally, the area of the solid material that crosses the REV (S_{ss}) is defined as in Eq. (9).

$$S_{SS} = \int_a^b h(x)dx \tag{9}$$

where $h(x)$ is a function that describes the profile of the 2D section representing the surface that crosses the REV boundary.

The methodology presented in this paragraph, applied repeatedly, can provide thermal conductivity at different instants during the sintering process. To obtain the thermal conductivity, in addition to the data relating to the material, the necessary information is the geometry of the neck between the particles. The neck geometry can be obtained from experimental methodologies or numerical models. The presented model is multiscale by definition because it starts from information on the neck dimension of a couple of powder particles and provides information about the complete powder bed at the macroscale level.

3 Results and discussion

As an example of the application of the methodology presented in Sect. 2, the thermal conductivity of a BCC structure made of nine powder particles was evaluated. Figure 2 shows the BCC cubic REV considered for the calculations.

Eight eighths of powder particles were considered centred at the edges of the cube. The diameter of these powder particles was considered constant and equal to 80 µm. A powder particle was considered at the centre of the REV. The diameter of this powder particle was assumed to be 58.6 µm. A particle with this diameter precisely fits the

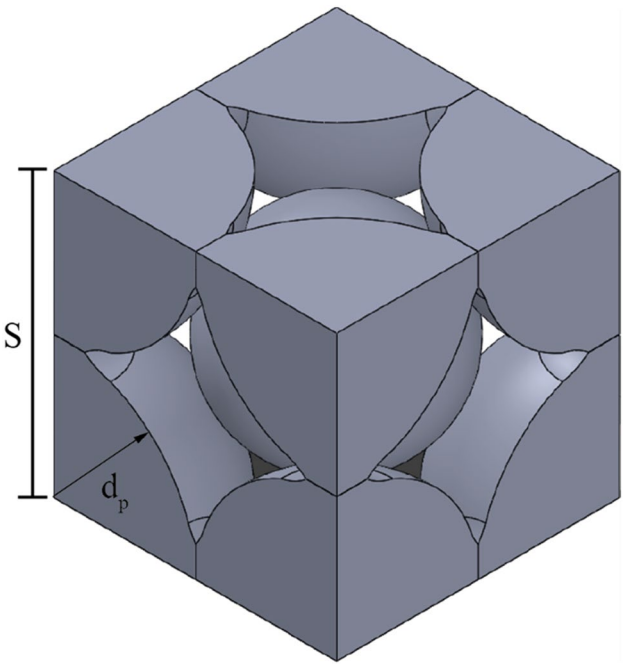

Fig. 2 REV with a BCC structure adopted to evaluate thermal conductivity. d_p represents the radius of the powder particle. S is the lateral size of the REV considered

vacuum at the centre of the structure. The diameters of the considered powder particles are comprised in the powder size distribution of 45–105 µm commonly processed during the PBF-EB process. Information about the neck and geometry evolution can be obtained from experimental data or numerical models. For the current work, geometrical information about the sintering powder particles was obtained using the model of sintering proposed by Rizza et al. [21]. According to this methodology, phase field simulations were performed under a temperature profile, which emulates the preheating step of the PBF-EB process. The temperature load consisted of a linear increase of the temperature in steps from 879 to 1273 K. Each simulation considered a couple of powder particles undergoing sintering due to only diffusion mechanisms, while the rigid body motion of the particles was neglected. More details about modelling can be found in Ref. [21]. The material considered was Ti6Al4V.

Table 1 summarizes the geometrical information for the neck among two powder particles with a diameter of 80 µm and the neck among the powder particles of 80 µm and 58.6 µm at different steps of the sintering simulation and different temperature conditions.

The total volume and the lateral surface of the REV were calculated considering the convex Hull geometry with the vertices placed at the centre of the considered powder particles. For this geometry, the total volume and the total surface of the REV were $U_0 = 512{,}000\ \mu m^3$ and $S_0 = 38{,}400\ \mu m^2$.

The geometrical information required to evaluate Eq. (4), Eqs. (5) and (6) were retrieved from Eq. (7), Eqs. (8) and (9), which summarised in Table 2, while n remains constant and equal to 0.75.

The geometrical information and the tortuosity factor in Table 2 were used to evaluate the thermal conductivity of the powder structure under consideration, from the bulk properties of the Ti6Al4V ($\lambda_{0,}$ α_0, ρ_0 and c_p), according to Eqs. 1 and 2.

Table 2 Geometrical information evaluated according to Eq. (7), Eqs. (8) and (9) and the tortuosity factor for the BCC REV under consideration

Time [s]	Temperature [K]	U_{0S} [µm^3]	S_{fs} [µm^2]	S_{SS} [µm^2]	τ [–]
0.5	879	380,954	30,442	30,530	2.39
1.5	913	380,449	30,726	31,150	2.39
2.5	964	380,239	31,408	31,570	2.43
3.5	1016	381,013	32,038	30,984	2.50
4.5	1050	381,653	32,662	32,174	2.53
5.5	1101	380,559	33,308	31,706	2.57
6.5	1153	382,206	34,302	31,619	2.80
7.5	1187	382,177	35,221	31,496	2.75
8.5	1239	382,709	36,283	31,334	2.85
9.5	1273	381,155	37,423	31,240	2.92

Table 3 reports the data of the bulk material and the corresponding thermal conductivity of the powder bed at different sintering conditions and temperatures of the system. Table 3 also includes the ratio between λ_0 e λ_{pow}. As can be observed, this ratio remains approximately constant during the sintering. A slight decrease is observed when the temperature rises. This result is justified by the fact that the densification mechanism due to the rigid body motion has been neglected. If the rigid body motion was present, under the temperature increase, the centres of the particles modify their position by approaching each other. The neck radius, therefore, would increase and the geometry of the structure would be slightly modified. Under this variation is excepted λ_{pow} to grow. Therefore, owing to the densification of the structure, it would be expected that the ratio λ_0/λ_{pow} slightly increases (or at least remains constant). This result is in agreement with the literature, where this ratio is usually assumed to be constant, e.g. Ref. [22]. In other cases, in the

Table 1 Geometrical information about the neck evolution of the couples 80–80 µm and the 80–58.6 µm powder particle, evaluated with the methodology proposed by Rizza et al. [21]

Couple of particles		80–80 µm			80–58.6 µm		
Time [s]	Temp [K]	x [µm]	$x+dx$ [µm]	h [µm]	x [µm]	$x+dx$ [µm]	h [µm]
0.5	879	3.84	7.02	0.80	4.26	5.93	0.70
1.5	913	5.40	9.01	1.40	5.31	6.17	0.92
2.5	964	6.31	10.08	1.78	5.96	7.98	1.33
3.5	1016	6.80	12.40	2.18	6.38	7.87	1.41
4.5	1050	7.28	10.79	1.87	6.70	8.95	1.77
5.5	1101	7.48	12.33	2.42	7.02	8.84	1.78
6.5	1153	7.95	13.48	2.53	7.25	9.61	2.14
7.5	1187	8.19	14.35	2.89	7.64	9.65	2.12
8.5	1239	8.42	15.24	3.10	7.90	10.42	2.50
9.5	1273	8.62	16.02	3.54	8.09	10.48	2.61

Table 3 Material properties adopted for the evaluation of thermal conductivity and the values of thermal conductivity for the powder bed (λ_{pow})

Time [s]	Temperature [K]	λ_0 [22] [$Wm^{-1}K^{-1}$]	α_0 [m^2s^{-1}]	c_p [22] [$Jkg^{-1}K^{-1}$]	ρ_0 [kgm^{-3}]	ρ_{pow} [kgm^{-3}]	α_{pow} [m^2s^{-1}]	λ_{pow} [$Wm^{-1}K^{-1}$]	λ_{pow}/λ_0 [–]
0.5	879	11.52	2.95×10^{-6}	912.53	4273.69	3180	9.19×10^{-7}	2.67	0.23
1.5	913	11.97	2.99×10^{-6}	937.61	4262.54	3167	9.30×10^{-7}	2.76	0.23
2.5	964	12.64	3.05×10^{-6}	975.24	4245.81	3153	9.34×10^{-7}	2.87	0.23
3.5	1016	13.33	3.11×10^{-6}	1013.61	4228.75	3146	9.25×10^{-7}	2.95	0.22
4.5	1050	13.78	3.14×10^{-6}	1038.69	4217.60	3143	9.26×10^{-7}	3.02	0.22
5.5	1101	14.45	3.20×10^{-6}	1076.32	4200.87	3122	9.24×10^{-7}	3.10	0.21
6.5	1153	15.14	3.25×10^{-6}	1114.68	4183.82	3137	8.71×10^{-7}	3.04	0.20
7.5	1187	15.59	3.28×10^{-6}	1139.77	4172.66	3115	8.89×10^{-7}	3.15	0.20
8.5	1239	16.27	5.31×10^{-6}	736.80	4155.61	3106	1.39×10^{-6}	3.19	0.20
9.5	1273	16.72	5.43×10^{-6}	743.6	4144.46	3085	1.38×10^{-6}	3.18	0.19

range of the investigated temperature in this work, calculating the powder properties via other modelling approaches, the ratio λ_0/λ_{pow} is a quite constant value, e.g. Ref. [7].

Numerically, the values of the thermal conductivity obtained with the proposed methodology were in the same order of magnitude of data available in the literature [7, 23–25]. Comparing the results with the ones reported in [7, 23–25], the values are slightly larger. However, the detected differences can be explained by considering the experimental conditions [23, 24] or the numerical approximations [7]. In fact, the analysis reported in Ref. [23, 24] refers to studies about the PBF process with a laser beam, which differs significantly from a PBF-EB, where the effect of the sintering cannot be neglected as in the case of Ref. [23, 24]. In Ref. [7], for simplicity, the neck has been assumed to be constant, neglecting the neck growth owed to the sintering phenomena.

As regards the data recently measured by Galati et al. [25], it was found that the thermal conductivity for the hollowed closed samples produced by PBF-EB and that contained inside sintered particles in vacuum varied approximately between 1.5 and 2.4 W/m^{-1} K^{-1} at 823 K and between 0.7 and 3.4 W/m^{-1} K^{-1} at 1023 K. These values, that more representative of the PBF-EB conditions (sintering, temperature and vacuum environment) were found in good agreement with the data obtained in this work.

4 Conclusions

The thermal conductivity of the powder bed during the PBF-EB process strongly influences the process conduction and the quality of the components produced. The current work proposed a novel methodology to evaluate the thermal conductivity of a powder bed, considering the peculiar evolution of the powder bed structure during the preheating phase of the PBF-EB process. Although this methodology was specifically designed 1for the PBF-EB process, it is applicable in general to all the powder beds. The information required to evaluate thermal conductivity, besides the information about the material, is the geometric information on the neck among the powder particles. This information can be obtained in several ways, such as experimentally or from numerical models.

The thermal conductivity of a BCC powder packing structure was evaluated as an application of the methodology developed. The BCC structure was selected because it is the most adopted in literature to represent the powder bed conditions during the PBF-EB process. The BCC structure was assumed to be made of nine spherical powder particles made of Ti6Al4V. Information about the neck growth and the geometry evolution were retrieved from phase field simulations conducted with the approach proposed by Rizza et al. [21].

For the BCC structure, the thermal conductivity was found to vary between 2.67 and 3.18 Wm^{-1} K^{-1}. These values of thermal conductivity were found to be in good agreement with the experimental data reported in the literature for PBF-EB. Different from the approaches available in the literature [25], the methodology presented in the current work allows the evaluation of thermal conductivity at different stages and conditions of the powder bed.

Future works should include densification of the structure and analyses of other powder bed structures to investigate the influence of the packing geometry on thermal conductivity.

Funding Open access funding provided by Politecnico di Torino within the CRUI-CARE Agreement.

Declarations

Competing interests On behalf of all authors, the corresponding author states that there is no conflict of interest.

References

1. Meier C, Weissbach R, Weinberg J et al (2019) Critical influences of particle size and adhesion on the powder layer uniformity in metal additive manufacturing. J Mater Process Technol 266:484–501. https://doi.org/10.1016/J.JMATPROTEC.2018.10.037
2. Jadhav SD, Vleugels J, Kruth JP et al (2020) Mechanical and electrical properties of selective laser-melted parts produced from surface-oxidized copper powder. Mater Des Process Commun 2:e94. https://doi.org/10.1002/MDP2.94
3. Luo Z, Zhao Y (2018) A survey of finite element analysis of temperature and thermal stress fields in powder bed fusion additive manufacturing. Addit Manuf 21:318–332. https://doi.org/10.1016/J.ADDMA.2018.03.022
4. Zhang S, Lane B, Whiting J, Chou K (2019) On thermal properties of metallic powder in laser powder bed fusion additive manufacturing. J Manuf Process 47:382–392. https://doi.org/10.1016/j.jmapro.2019.09.012
5. Masoomi M, Gao X, Thompson SM, et al (2016) Modeling, simulation and experimental validation of heat transfer during selective laser melting. ASME Int Mech Eng Congr Expo Proc 2A. https://doi.org/10.1115/IMECE2015-52165
6. Galati M, Rizza G, Defanti S, Denti L (2021) Surface roughness prediction model for Electron Beam Melting (EBM) processing Ti6Al4V. Precis Eng 69:19–28. https://doi.org/10.1016/j.precisioneng.2021.01.002
7. Galati M, Iuliano L, Salmi A, Atzeni E (2017) Modelling energy source and powder properties for the development of a thermal FE model of the EBM additive manufacturing process. Addit Manuf 14:49–59. https://doi.org/10.1016/j.addma.2017.01.001
8. Yan W, Ge W, Smith J et al (2016) Multi-scale modeling of electron beam melting of functionally graded materials. Acta Mater 115:403–412. https://doi.org/10.1016/J.ACTAMAT.2016.06.022
9. Gusarov AV, Laoui T, Froyen L, Titov VI (2003) Contact thermal conductivity of a powder bed in selective laser sintering. Int J Heat Mass Transf 46:1103–1109. https://doi.org/10.1016/S0017-9310(02)00370-8
10. Presley MA, Christensen PR (1997) Thermal conductivity measurements of particulate materials 1. A review. J Geophys Res E Planets 102:6535–6549. https://doi.org/10.1029/96JE03302
11. Gong X, Cheng B, Price S, Chou K (2013) Powder-bed electron-beam-melting additive manufacturing: powder characterization, process simulation and metrology. In: ASME Early Career Technical Conference Birmingham, AL, USA, District F, Section 2, pp 59–66
12. Smith CJ, Tammas-Williams S, Hernandez-Nava E, Todd I (2017) Tailoring the thermal conductivity of the powder bed in Electron Beam Melting (EBM) Additive Manufacturing. Sci Rep 7:1–8. https://doi.org/10.1038/s41598-017-11243-8
13. Leung CLA, Tosi R, Muzangaza E et al (2019) Effect of preheating on the thermal, microstructural and mechanical properties of selective electron beam melted Ti-6Al-4V components. Mater Des 174:107792. https://doi.org/10.1016/J.MATDES.2019.107792
14. Neira Arce A (2012) Thermal modeling and simulation of electron beam melting for rapid prototyping on Ti6Al4V Alloys. Dissertation, North Carolina State University, Raleigh
15. Chua BL, Lee HJ, Ahn DG (2018) Estimation of effective thermal conductivity of Ti-6Al-4V powders for a powder bed fusion process using finite element analysis. Int J Precis Eng Manuf 192(19):257–264. https://doi.org/10.1007/S12541-018-0030-2
16. Grose J, Cullinan M, Dibua OG, et al (2021) Simulation and characterization of nanoparticle thermal conductivity for a microscale selective laser sintering system. Proceedings of ASME 2021 16th Int Manuf Sci Eng Conf MSEC 2021 2. https://doi.org/10.1115/MSEC2021-64048
17. Ahmadi MM, Mohammadi S, Hayati AN (2011) Analytical derivation of tortuosity and permeability of monosized spheres: a volume averaging approach. Phys Rev E Stat Nonlinear Soft Matter Phys 83:1–8. https://doi.org/10.1103/PhysRevE.83.026312
18. Montes JM, Cuevas FG, Cintas J (2007) Electrical and thermal tortuosity in powder compacts. Granul Matter 9:401–406. https://doi.org/10.1007/s10035-007-0061-3
19. Cooper SJ, Bertei A, Shearing PR et al (2016) TauFactor: an open-source application for calculating tortuosity factors from tomographic data. SoftwareX 5:203–210. https://doi.org/10.1016/J.SOFTX.2016.09.002
20. Mordukhovich BS, Mau Nam N (2022) Convex analysis and beyond. Springer International Publishing, Cham
21. Rizza G, Galati M, Iuliano L (2022) A phase-field study of neck growth in electron beam powder bed fusion (EB-PBF) process of Ti6Al4V powders under different processing conditions. Int J Adv Manuf Technol 123:855–873. https://doi.org/10.1007/s00170-022-10204-4
22. Qi HB, Yan YN, Lin F, Zhang RJ (2007) Scanning method of filling lines in electron beam selective melting. Proc Inst Mech Eng Part B J Eng Manuf 221:1685–1694. https://doi.org/10.1243/09544054JEM913
23. Zhang S, Lane B, Whiting J, Chou K (2020) An investigation into metallic powder thermal conductivity in laser powder bed fusion additive manufacturing. In: Solid Freeform Fabrication 2018: Proceedings of the 29th Annual International Solid Freeform Fabrication Symposium—An Additive Manufacturing Conference, SFF 2018. pp 1796–1807
24. Liu M, Chiu LNS, Shen H et al (2022) Effective thermal conductivities of metal powders for additive manufacturing. Powder Technol 401:117323. https://doi.org/10.1016/J.POWTEC.2022.117323
25. Galati M, Campagnoli E, Giaretto V, Iuliano L (2023) Modelling the thermal behaviour of Ti6Al4V sintered powder bed in electron beam powder bed fusion (EB-PBF). Procedia CIRP 118:664–669. https://doi.org/10.1016/J.PROCIR.2023.06.114